RELATIVE IMPORTANCE OF OPTICAL FIBER EFFECTIVE AREA AND ATTENUATION IN SPAN LENGTH OPTIMIZATION OF ULTRA-LONG 100 GBPS PM-QPSK SYSTEMS

William A. Wood, Sergey Ten, Ioannis Roudas, Petr M. Sterlingov, Nikolay A. Kaliteevskiy, John D. Downie, and Margarita Rukosueva (Corning Incorporated).
Email: woodwa@corning.com

Corning Incorporated
SP-TD-01-1
One Riverfront Plaza
Corning, New York 14831 USA

Abstract: We investigate the performance of very long submarine 100 Gbps PM-QPSK WDM systems as a function of the span length, attenuation and effective area (Aeff) of optical fiber. It is determined that the optimal span length is independent of fiber Aeff and is longer for fibers with ultra-low attenuation. We show that for two fibers with the same performance in a 50 km span system, the fiber with lower attenuation will perform better in systems with longer spans, enabling higher margin, longer reach, or increased spectral efficiency with fewer repeaters.

1. Introduction

There is considerable interest in extending 100G polarization multiplexed quaternary phase-shift keyed (PM-QPSK) wavelength-division-multiplexed (WDM) transmission systems to submarine distances that cover all practical intercontinental routes. Loop experiments demonstrating reaches up to 14,000 km EDFA-only transmission have been described, and in other experiments spectral efficiencies up to 4.0 b/s/Hz have been reported.[1] Typically, these experiments are performed with short (e.g., 50 km) span lengths, since it is known that up to a certain limit, shorter span lengths increase system reach.

It is interesting to explore the extent to which ultra-low-loss fibers with large Aeff fiber can enable a reduction in the number of repeaters. In this paper, the performance of fixed-reach, 100G PM-QPSK WDM systems and its dependence on span length is investigated. Three transmission fibers with different Aeffs and attenuation coefficients at reaches of 6,000, 9,000 and 12,000 km are considered.

Fiber A has the lowest attenuation and a large Aeff (see Table 2); it generally outperforms the other two fibers. Fibers B and C perform similarly in the 50 km span systems. Fiber C has a larger Aeff than Fiber B, but also has higher attenuation. It is interesting to study how the relative advantages of these fibers can be exploited to reduce the number of repeaters, increase overall reach, or increase the spectral efficiency (SE), depending on the application requirements. Hence, the ideal span length, optimal channel power and system performance at various reaches and spectral efficiencies are studied for these three fibers.

2. Simulation Description

This article describes simulations of an eight-channel, 100 Gbps, 28 Gbaud PM-QPSK transmission systems with 50 GHz channel spacing. A schematic of the system is shown in Fig. 1.

The transmitter model includes electrical low-pass filters (LPF) at the input of the modulators to emulate devices with limited electrical bandwidth. The transmitter parameters are shown in Table 1.
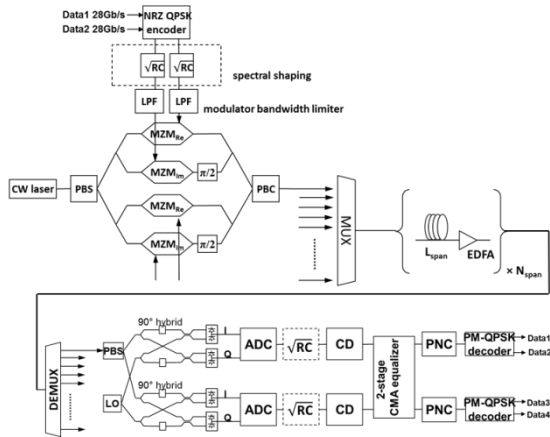

Fig. 1. A diagram of the PM-QPSK system. A low-pass filter (LPF) is added to model the electrical bandwidth limitations of real modulators. (key: NRZ = non-return-to-zero, MZM = Mach-Zehnder modulator, CW = continuous wave, PBS/C = polarization beam splitter/combiner). Spectral shaping is discussed in Section 4. MZMs in the transmitter that modulate second polarization are identical to Data1 and Data2 and are omitted for simplicity.

As illustrated in Fig. 2, the electrical filter bandwidths are chosen to match the modeled back-to-back OSNR sensitivity to recently published data. [2]

Table 1. System modeling parameters

	Unit	Value
Laser linewidths	kHz	100.0
Electrical LPF bandwidth	GHz	18.0
Optical MUX/DEMUX LPF FWHM	GHz	28.0
Number of symbols	-	32767
RX sampling rate	GSa/s	40.0
CMA taps	-	11
ADC bits	-	6

Our receiver model contains a two-stage "constant modulus algorithm" equalizer [3] and a phase noise compensator [4]. Other receiver parameters are listed in Table 1. The bit error rate is estimated from the received constellation using a stochastic, semi-analytic method [5].
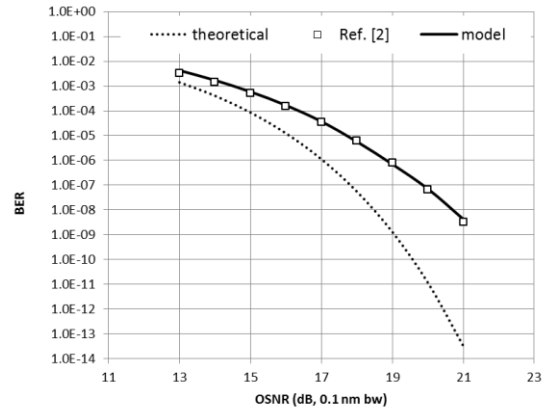

Fig. 2. Back-to-back BER vs. OSNR.

A split-step Fourier method [6,7] is used to solve the polarization-resolved nonlinear Schrödinger equation appropriate for modeling transmission in optical fiber. We consider three different optical fibers in this study. The first two are pure silica core optical fibers, and the third is a germanosilicate fiber.

Table 2. Fiber model parameters

	Fiber A	Fiber B	Fiber C
Aeff (μm^2)	150	112	155
Attenuation (dB/km)	0.155	0.158	0.185
Dispersion (ps/nm/km)	20.9	20.35	21.7
n2 (m^2/W)	2.10E-20	2.10E-20	2.30E-20

Table 2 describes the parameters of optical fibers in our modeling except common parameters that are dispersion slope (0.06 ps/nm²/km) and PMD coefficient (0.03 ps/√km)

We consider amplifier spans of 10, 20, 30, 35, 40, 50, 60, 80 and 100 km constructed with these fibers, amplified by erbium-doped fiber amplifiers (EDFAs) with a 5 dB noise figure, independent of span length.

3. Results and Discussion

The performance of 6,000, 9,000 and 12,000 km PM-QPSK systems is simulated as a function of span length. We start by calculating Q versus input power per channel for each span length and fiber

type. Example results are shown in Fig. 3. For each span length, we obtain concave curves of the functional form:

$$Q^2(P) = \frac{P}{\alpha + \beta P^3} \qquad (1)$$

where α and β are parameters related to the amplified spontaneous emission (ASE), and effective nonlinear noise variances, respectively. The parameter α does not contain fiber attributes related to nonlinearity (n_2/Aeff).[8] Using this functional form to fit the data, we obtain the maximum Q and optimal launch power for each span length.

Fig. 3 shows that for each span length, the variation of Q near its maximum is shallow. If we expand Eqn. 1 to second order in power deviation about the optimal ($\Delta P = P - P_0$), we obtain the simple formula

$$Q^2/Q_0^2 = 1 - \Delta P^2/P_0^2 . \qquad (2)$$

Hence, power per channel reduction of 1.2 and 1.75 dB from optimal will result in Q^2 reduction of only 0.25 and 0.5 dB respectively. This behavior is very different from the linear regime where a 1 dB reduction in channel power usually leads to 1 dB reduction in Q^2.
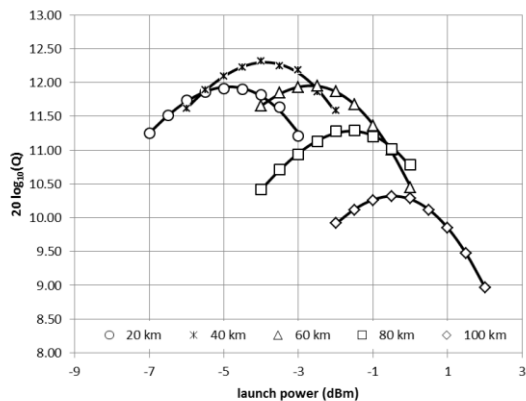

Fig. 3. Fiber B system Q factor vs. launch power for 9,000km reach and span lengths ranging from 20 to 100 km. Markers correspond to Monte Carlo simulations, and the curves are fit.

Representing the Q parameter as in Eqn. 1, we find the optimal power and Q values are given by:

$$P_0 = \sqrt[3]{\alpha/2\beta}, \quad Q_0^2 = \frac{2}{3}\left[\alpha^2\beta\right]^{-1/3} \qquad (3)$$

Then, according to [8], the dependence of Q_0 on Aeff comes entirely through the nonlinear noise coefficient β. We have, from [8]:

$$\beta \propto A_{eff}^{-2}, \text{ hence } Q_0^2 \propto A_{eff}^{2/3} \text{ and } P_0 \propto A_{eff}^{2/3} \quad (4)$$

This simple argument implies that the optimal Q and the optimal launch power for Fiber A should both be 0.85 dB higher than for Fiber B as the fibers differ mainly in Aeff. This agrees reasonably well with our calculations.

Fig. 4 illustrates the performance as a function of reach for fixed span lengths of 50km. The performance of Fibers B and C is nearly identical. Fiber A supports additional 2000 km transmission distance if we assume that Q^2=12.5 dB as a desired operating point with sufficient margin over hard decision FEC.

However, realizing the advantage of large Aeff fiber requires higher optical power. Fig. 4 also shows the optimal launch powers (right axis). For example Fiber A requires a power per channel of -2.5 dB (16.5 dBm for 80 channels) to achieve 0.85 higher Q than Fiber B operating at a total power of 16 dBm. However, given the shallow dependence of Q versus channel power, the Q margin available over minimum required Q could be exchanged to lower the channel power. For example, if Fiber A has excess 0.5 dB Q margin, then according to Eqn. 2, the power per channel can be lowered by 1.75 dB to bring Q to the minimally required level and lower the total power requirement for the amplifier to 14.75 dBm. For the same Q performance as Fiber B, Fiber C requires almost 1.6 dB higher

power per channel and approximately 17.5 dBm total power.

We observe that the optimal powers do not change significantly with reach, particularly at 6,000 km or larger. This is consistent with Eqn. 3 because, according to [8], α is exactly and β is approximately proportional to the number of spans, so the dependence of $P_0 = \sqrt[3]{\alpha/2\beta}$ on reach nearly cancels out. In fact, the simulations suggest a slight decrease in power with reach. Because the optimal power does not change appreciably, the additional Q margin available in shorter lengths e.g. 6000 km can be used to operate the system at sub-optimal (lower) channels powers consistent with Eqn. 2 This would significantly reduce the requirement for total power. Alternatively, if the total available EDFA power is sufficient, the additional Q margin can be used to extend the amplifier spacing, thus reducing the number of expensive repeaters and improving the overall system reliability.

The dependence of maximum Q on span length in a 9,000 km system is shown in Fig. 5. Fibers B and C exhibit equivalent performance at 50 km span lengths, and Fiber A exceeds the other two in performance at all span lengths.
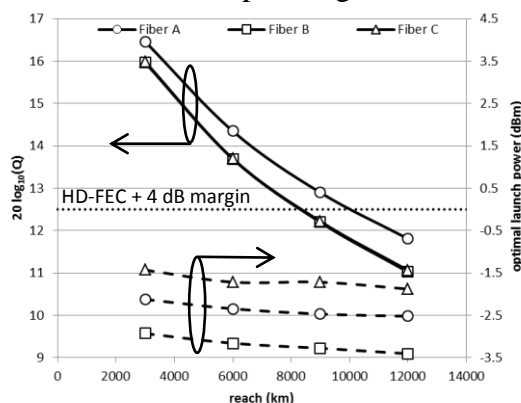

Fig. 4. Maximum Q vs. reach and optimal launch power vs. reach for 50 km spans. Fibers B and C have nearly identical Q curves. The dotted line at Q = 12.5 dB corresponds to the hard-decision FEC threshold plus 4 dB margin. (key: A = circles, B = squares, and C = triangles)
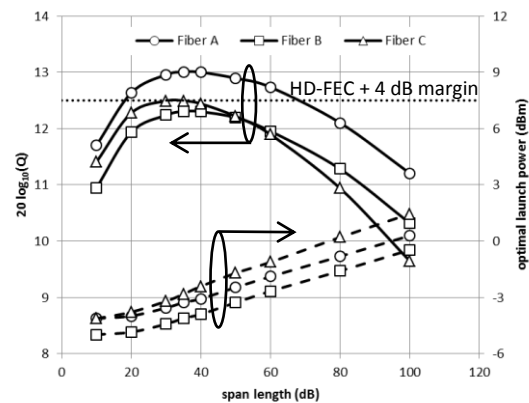

Fig. 5 Maximum Q vs. span length for three fibers in a 9,000 km link, SE 2 b/s/Hz. The dotted line at Q = 12.5 dB corresponds to the hard-decision FEC threshold plus 4 dB margin. (key: A = circles, B = squares, and C = triangles).

Table 3 Peak change in Q values in dB for three fibers and three reaches, relative to 9,000 km

	A	B	C
6,000 km	1.4	1.5	1.5
9,000 km	0	0	0
12,000 km	-1.1	-1.1	-1.1

It may be observed that in Fig. 5, the optimal span length is the same for Fibers A and B. Their attenuation coefficients are nearly the same, but their Aeffs are substantially different. On the other hand, A and C have nearly the same Aeffs, but their attenuations are different. Hence, one may conclude that the optimal span length depends only on fiber attenuation, at least for the Aeff ranges examined in this paper. Indeed from the equations in [8] the following approximate relationship can be derived:

$$L_{span,opt} \approx \frac{3}{2\alpha}\left(1 - \frac{e^{-3/2}}{F}\right) \qquad (4)$$

where α is the attenuation and F is the EDFA noise figure. It shows that optimal span length depends only on the attenuation and EDFA noise figure.

This has important consequences for fiber design. The shortest spans used in submarine systems are forty to fifty kilometers. Achieving attenuation similar to that of fibers A and B insure that at those span lengths, the transmission

---

systems are extremely close to their maximum performance.

It is important to notice the shallow dependence of Q as function of span length near the maximum value. This provides an important cost reduction opportunity to increase the span length using fibers with larger Aeff, although higher power amplifiers are required. For instance in Figure 5 Fiber A reaches minimal required Q at the span length of 70 km thus decreasing the number of amplifiers by 40% compare to the system with 50 km. This span length increase does require higher power per channel of -1 dBm and total EDFA power of 18 dBm compared to the power of 14.75 dBm that is required to reach a minimum required Q for Fiber B with 50 km span. Thus, Fiber A gives a system designer a choice of using the extra margin through either longer span length or lower power EDFA.

4. Higher Spectral Efficiency

In addition to 50 GHz, we considered channel spacings of 33.0, and 28.57 GHz, corresponding to spectral efficiencies of 3.03 and 3.5 b/s/Hz respectively. To control ISI, we use spectral shaping via a square root, raised-cosine filter in the transmitter and a matched filter in the receiver. The raised-cosine roll-off parameter [9] we use is 0.1.
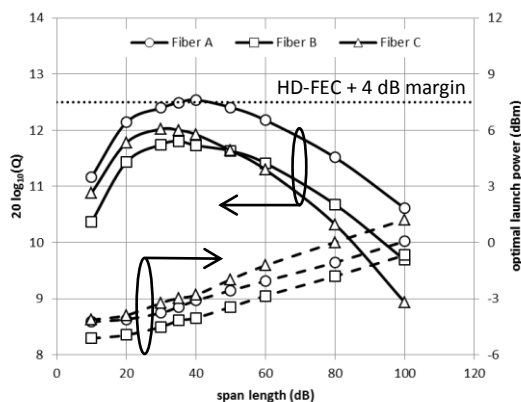

Fig. 6. Q vs. span length for three fibers in a 9,000 km link at 3 b/s/Hz SE. (key: A = circles, B = squares, and C = triangles)

At an SE of 3 b/s/Hz, the shape of the $Q(P_{ch})$ curves is essentially unchanged from 2 b/s/Hz. The 9,000 km results are summarized in Fig. 6. The performance of the 50 km spans versus reach at 3 b/s/Hz in Fig. 7 is quite similar to that at 2 b/s/Hz. For all fibers, there is a 0.25 dB approximate penalty at 3,000 km, increasing to approximately 0.5 dB at 12,000 km.
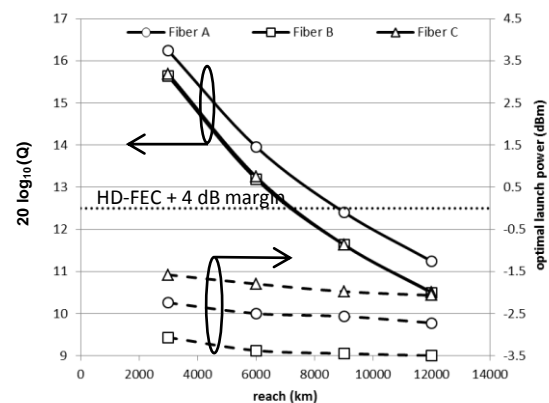

Fig. 7. Q vs. reach and optimal launch power vs. reach for 50 km spans, SE 3 b/s/Hz.

Fig. 8 shows the performance of the three fibers at 9000 km as a function of SE. There is about 1 dB drop in performance, uniformly across all fiber types, as SE is increased from 2 to 3.5 b/s/Hz with the aid of spectral shaping. We do not observe any difference in the relative behavior of the fiber types at higher SE. However, because the achieved Q factor of Fiber A is about 0.85 dB higher than the others, Fiber A could be operated at an SE exceeding 3 b/s/Hz and provide the same Q performance as the other fibers at 2 b/s/Hz.

5. Conclusion

In this paper we investigated the performance of very long submarine 100 Gbps PM-QPSK WDM systems on span length, attenuation and Aeff of optical fiber. We considered three representative length (6000, 9000 and 12000 km) covering the possible range of very long submarine systems and range of spectral efficiencies from 0.2 to 3.5 b/s/Hz.
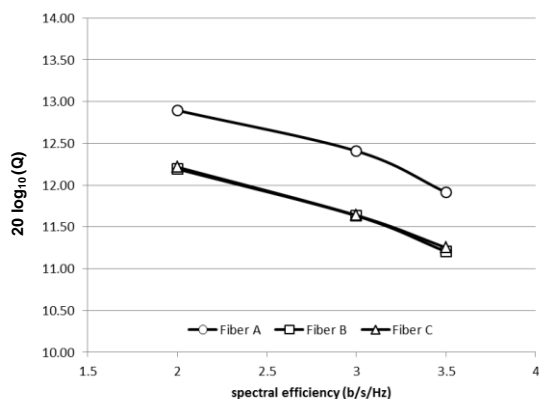
Fig. 8. Q vs. SE for 9,000 km, in 50 km spans. Fibers B and C show nearly identical performance.

By varying the span length at the fixed system reach for three representative fibers, we found that the optimal span length does not depend on Aeff. For pure silica core fibers with ultra low attenuation, the optimal span lengths is 40 km. However, in general, the dependence of Q as a function of span length is rather shallow, hence practical systems with 50 km spans incur only 0.2 dB penalty for those fibers. We found that larger Aeff increases Q for all span lengths and that has important implications for system design.

First, it may create an additional system margin that can be used to operate the system at suboptimal channel power, decreasing amplifier total output power requirements. Second, this higher margin may be used to extend the span length significantly (e.g. in our example 40%) thus decrease the number of repeaters albeit with higher required amplifier output power. Third, this extra margin may be used to deploy a system with higher spectral efficiency. In our simulations increase in spectral efficiency from 2 to 3.5 b/s/Hz resulted in additional 1 dB penalty in Q.

Finally, the ultra-low attenuation, large-effective-area pure silica core fibers provide the longest reach at practical 50 km span lengths; the optimal span length of 40 km would enable a maximum performance that is only 0.2 dB higher at a hefty cost of 20% more repeaters.

6. References

[1] J.-X. Cai, et al, "Transmission of 96 100-Gb/s Bandwidth-Constrained PDM-RZ-QPSK Channels With 300% Spectral Efficiency Over 10610 km and 400% Spectral Efficiency Over 4370 km" IEEE J. Lightwave Technol., 29(4) pp. 491-498. 2011.

[2] M. Salsi, et al. "WDM 200Gb/s Single-Carrier PDM-QPSK Transmission over 12,000km," ECOC 2011, paper Th.13.C.5.

[3] Chongjin Xie and S. Chandrasekhar, "Two-Stage Constant Modulus Algorithm Equalizer for Singularity Free Operation and Optical Performance Monitoring in Optical Coherent Receiver," OFC 2010, paper OMK3.

[4] Viterbi et al, "Nonlinear Estimation of PSK-Modulated Carrier Phase with Application to Burst Digital Transmission", IEEE Trans. Information Theory, vol. IT-29, no. 4, July 1983.

[5] X. Zhu, I. Roudas, J. Cartledge, "Error probability estimation for coherent optical PDM-QPSK communications systems," Proceedings of SPIE 8309, 830939, 2011.

[6] G. Strang, On the construction and comparison of difference schemes, SIAM J. Numer. Anal. 5 (1968), 506–517.

[7] J.A.C. Weideman, B.M. Herbst, Split-step methods for the solution of the nonlinear Schrödinger equation, SIAM J. Numer. Anal. 23 (1986), 485–507.

[8] G. Bosco, et al. "Analytical results on channel capacity in uncompensated optical links with coherent detection," Opt. Expr., Vol. 19, pp. B438–B449, 2011.

[9] J.G. Proakis, M. Salehi, *Digital Communications, 5th edition*, (McGraw-Hill, New York, 2008) eqn 9.2-26, pp. 607.